Journal of Alloys and Compounds 521 (2012) 106–111

Contents lists available at SciVerse ScienceDirect

Journal of Alloys and Compounds

journal homepage: www.elsevier.com/locate/jallcom

Proton and oxide-ion conduction in ZnO doped SnP_2O_7 ceramics

Jia Xiao, Hongmin Zhang, Zhijie Yang, Hongtao Wang, Guilin Ma*, Zhufa Zhou**

Key Laboratory of Organic Synthesis of Jiangsu Province, College of Chemistry, Chemical Engineering and Materials Science, Soochow University, Suzhou 215123, China

ARTICLE INFO

Article history:
Received 17 November 2011
Received in revised form 10 January 2012
Accepted 10 January 2012
Available online 28 January 2012

Keywords:
Tin pyrophosphate
Ionic conduction
Conductivity
Isotope effect
Gas concentration cell

ABSTRACT

A series of $Sn_{1-x}Zn_xP_2O_7$ (x = 0, 0.03, 0.06, 0.09, 0.12) ceramic samples have been prepared by a conventional solid state reaction method. The ceramic samples of x = 0.00–0.09 exhibited a single phase structure, and the doping limit of Zn^{2+} in SnP_2O_7 was at least x = 0.09. The conduction behaviors of the ceramic samples were investigated by means of electrochemical methods including AC impedance spectroscopy, isotope effect, gas concentration cells etc. in the temperature range of 300–650 °C. Among the ceramic samples studied, the highest conductivities were observed for the $Sn_{0.91}Zn_{0.09}P_2O_7$ sample to be 1.69×10^{-4} S cm^{-1} in wet air and 1.91×10^{-4} S cm^{-1} in wet hydrogen at 600 °C. Isotope effect confirmed the ceramic samples possessed proton conduction under water vapor-containing atmosphere. It was found that the sintering temperature of 1200 °C in present investigation could result in not only appropriate densities, but also high conductivities of ceramic samples. It was also found that in wet hydrogen atmosphere $Sn_{0.91}Zn_{0.09}P_2O_7$ was almost a pure ionic conductor, the ionic conduction was contributed mainly to proton and partially to oxide-ion, whereas in wet air atmosphere, the ceramic sample exhibited a mixed ion and electron hole conduction.

1. Introduction

Fuel cell as a promising alternative power generation system has excited worldwide attention for the conversion of chemical energy directly and cleanly into electrical power with high efficiency. A crucial requirement for such power generation system is a good ionic conductor as the electrolyte [1–3]. Traditionally, high temperature electrolyte materials, such as doped $BaCeO_3$, $LaGaO_3$ and yttria-stabilized zirconia (YSZ) etc., are commonly operated at temperature range above 600 °C [4–8]. However, relatively high operating temperature limits material selectivity, increases material degradation, shortens material lifetime, augments cost and slows down the commercialization of fuel cell [9]. In comparison, intermediate temperature fuel cells can combine many merits of high temperature and low temperature fuel cells. They allow extensive material selectivity, fast reaction kinetics and diffusion rates, reduction of electrocatalyst loading, improved tolerance for fuel impurities of CO, etc., and easy heat and water management [10,11]. Therefore, exploitation for intermediate temperature (100–600 °C) electrolyte materials for fuel cells has become a crucial goal for the next generation of fuel cell technology [3]. Some oxo acid salts, for example, $CsHSO_4$ [2] and CsH_2PO_4 [12,13] have high proton conductivities at intermediate temperatures. The former has not only high proton conductivity (8×10^{-3} S cm^{-1}, at 150 °C), but also high stability below 250 °C. The H_2/O_2 fuel cell using $CsHSO_4$ solid electrolyte exhibits promising electrochemical performances with open circuit voltages of 1.11 V and current densities of 44 mA·cm^{-2} at short circuit. But $CsHSO_4$ is unstable above 250 °C. More recently, it has been reported that the tin pyrophosphate (SnP_2O_7) doped with tri- or divalent cations (Ga^{3+}, Sc^{3+}, Sb^{3+}, Al^{3+}, In^{3+} and Mg^{2+}, etc.) on Sn^{4+} site shows high proton conductivities in the temperature range of 100–400 °C under unhumidified conditions [11,14–19]. However, it should be kept in mind that samples in these previous studies were prepared by merely pressing SnP_2O_7-based powders into pellets and the heat-treated temperatures were all less than 700 °C. Until now, only a few papers dealt with the preparation of SnP_2O_7-based ceramic pellets through sintering procedure [20–22]. Tao [21] reported that $Sn_{0.92}In_{0.08}P_2O_{7-\delta}$ ceramic pellet was prepared by an aqueous solution route and a single phase pyrophosphate was formed by sintering the green pellet at 1000 °C, giving a conductivity of 8×10^{-9} S cm^{-1} at 400 °C in air. Phadke et al. [22] reported that dense $Sn_{0.9}Zn_{0.1}P_2O_{7-\delta}$ ceramic pellet was obtained through sintering the green pellet at 1400 °C, and that $Sn_{0.9}Zn_{0.1}P_2O_{7-\delta}$ showed a conductivity of 2.84×10^{-6} S cm^{-1} at 600 °C in unhumidified air. These conductivity values are several orders of magnitude lower than the previously reported conductivity values for unsintered pellets prepared merely by pressing the doped tin pyrophosphate powders [14–18]. The presence of leftover phosphoric acid in the unsintered pellets is responsible for the high conductivity values for the unsintered pellets [22,23]. Hibino et al. [24,25] reported a SnP_2O_7–SnO_2 composite ceramic

* Corresponding author. Tel.: +86 512 65880326; fax: +86 512 65880089.
** Corresponding author. Tel.: +86 512 65880326; fax: +86 512 65880089.
E-mail address: 32uumagl@suda.edu.cn (G. Ma).

0925-8388/$ – see front matter © 2012 Elsevier B.V. All rights reserved.
doi:10.1016/j.jallcom.2012.01.058

exhibited relatively high proton conductivities in the temperature range of 100–700 °C. It seems that the performance of SnP_2O_7-based ceramic materials is highly dependent upon the prepared route used.

However, the investigation on conduction in $Sn_{0.9}Zn_{0.1}P_2O_{7-\delta}$ reported by Phadke et al. [22] is insufficient. In addition, effect of Zn^{2+} doping level on phase purity and electrochemical properties of Zn^{2+}-doped SnP_2O_7 has not yet been investigated. In this study, a series of ceramic samples $Sn_{1-x}Zn_xP_2O_7$ (x = 0, 0.03, 0.06, 0.09, 0.12) were prepared, the microstructures and electrochemical properties were explored.

2. Experimental

2.1. Preparation and characterization

Ceramic samples $Sn_{1-x}Zn_xP_2O_7$ (x = 0, 0.03, 0.06, 0.09, 0.12) were prepared by a conventional solid state reaction method. The required amounts of SnO_2 (Luoyang Ship Material Research Institute, 50–70 nm), ZnO (99.0%) and 85% H_3PO_4 were fully mixed and held with stirring around 350 °C until they became solid mixtures. The H_3PO_4/(SnO_2 and ZnO) molar ratio was controlled to be 3.0 in order to compensate phosphorus loss by vaporization during the heating process [22]. The solid mixtures were then calcined in a covered alumina crucible for 2 h at 600 °C. The calcined powders were ground, followed by sieving (100 mesh). The resulting powders were pressed into pellets at hydrostatic pressure of 300 MPa, and sintered at 1200 °C for 5 h. The crystalline structures of the obtained ceramic samples were determined by powder X-ray diffraction (XRD) analysis using a nickel filtered Cu K_α (λ = 1.5405 Å) radiation on a Panatytical X' Pert Pro MPD X-ray diffractometer. The scanning range and rate were 15–80° and 2.00° min^{-1}, respectively. Microstructures of fracture surfaces of the ceramic samples were observed by scanning electron microscope (SEM). Total linear shrinkage ($(l_o - l)/l_o$, where l_o is the initial length and l is the final length), resulting from sintering was established from direct measurements of sample dimensions before and after sintering. The relative densities of the sintered pellets were determined by geometrical measurements.

2.2. Electrochemical measurements

The ceramic pellets were made into thin discs (diameter 17 mm, thickness 0.8–1.0 mm) to serve as electrolytes. Platinum paste was painted on two surfaces of each disc to serve as electrode, and dried by infrared lamp. Platinum guaze was attached to the electrode surfaces and connected to Pt wires (diameter 0.5 mm). The as-prepared testing sample was sealed by Pyrex glass sealing ring between two alumina tubes, placed into an electric furnace and then fired at 900 °C for 20 min. The conductivities were measured by an AC impedance method using electrochemical workstations (German Zahner IM6ex) in the temperature range of 300–650 °C, in wet air and wet hydrogen atmospheres, respectively. A frequency range from 1 Hz to 3 MHz and a voltage amplitude 50 mV were applied. The wet experimental gas was obtained by bubbling of gas through water at 25 °C. To verify the proton conduction in water vapor-containing atmosphere, the conductivity was measured under H_2O–Ar (Ar saturated with water vapor at 25 °C) and D_2O–Ar (Ar saturated with heavy water vapor at 25 °C) atmospheres.

For investigation of the ionic conduction properties in wet hydrogen atmosphere, hydrogen and water vapor concentration cells were fabricated. The cells using typical $Sn_{0.91}Zn_{0.09}P_2O_7$ ceramic sample as an electrolyte are expressed as follows:

$$H_2(P_{H_2} = 1.01\times10^5\ \text{Pa})(p_{H_2O} = 3.40\times10^3\ \text{Pa}),\ Pt|Sn_{0.91}Zn_{0.09}P_2O_7|Pt,H_2\text{–}Ar(p_{H_2} = 5.05\times10^3\ \text{Pa})(p_{H_2O} = 3.40\times10^3\ \text{Pa}) \quad (1)$$

$$H_2(P_{H_2} = 1.01\times10^5\ \text{Pa})(p_{H_2O} = 3.40\times10^3\ \text{Pa}),\ Pt|Sn_{0.91}Zn_{0.09}P_2O_7|Pt,H_2(p_{H_2} = 1.01\times10^5\ \text{Pa})(p_{H_2O} = 1.23\times10^4\ \text{Pa}) \quad (2)$$

The observed values (EMF_{obs}) of electromotive forces can be expressed as [26],

$$EMF_{obs} = \frac{RT}{2F}\left\{-t_{ion}\ln\left[\frac{p_{H_2}(II)}{p_{H_2}(I)}\right] + t_O\ln\left[\frac{p_{H_2O}(II)}{p_{H_2O}(I)}\right]\right\}$$

Where $P_{H_2}(II)$, $P_{H_2O}(II)$, $P_{H_2}(I)$, $P_{H_2O}(I)$ represent the partial pressures of hydrogen gas and water vapor in each side of chambers, respectively. If the P_{H_2} in each chamber is the same, i.e. $P_{H_2}(I) = P_{H_2}(II)$, the EMF of water vapor concentration cell gives the transference number of oxide-ion (t_O). Likewise, the EMF of hydrogen concentration cell with $P_{H_2O}(I) = P_{H_2O}(II)$ gives the sum of the proton and oxide-ion contributions.

The total ionic transference number ($t_{ion} = t_H + t_O$) can be obtained by EMF_{obs}/EMF_{cal}, where EMF_{cal} is the theoretical, given by the Nernst equation,

$$EMF_{cal} = \frac{RT}{2F}\ln\left[\frac{pH_2(II)}{pH_2(I)}\right]$$

Similarly, the ionic conduction properties in wet air were determined through the following oxygen and water vapor concentration cells (3) and (4),

$$Air(P_{O_2} = 2.12\times10^4\ \text{Pa})(p_{H_2O} = 3.40\times10^3\ \text{Pa}),\ Pt|Sn_{0.91}Zn_{0.09}P_2O_7|Pt,O_2(p_{O_2} = 1.01\times10^5\ \text{Pa})(p_{H_2O} = 3.40\times10^3\ \text{Pa}) \quad (3)$$

$$O_2(P_{O_2} = 1.01\times10^5\ \text{Pa})(p_{H_2O} = 1.23\times10^4\ \text{Pa}),\ Pt|Sn_{0.91}Zn_{0.09}P_2O_7|Pt,O_2(p_{O_2} = 1.01\times10^5\ \text{Pa})(p_{H_2O} = 3.40\times10^3\ \text{Pa}) \quad (4)$$

The observed values (EMF_{obs}) of electromotive forces are given by following Nernst equation [26],

$$EMF_{obs} = \frac{RT}{4F}\left\{t_{ion}\ln\left[\frac{p_{O_2}(II)}{p_{O_2}(I)}\right] - 2t_H\ln\left[\frac{p_{H_2O}(II)}{p_{H_2O}(I)}\right]\right\}$$

The EMF of oxygen concentration cell with $P_{H_2O}(I) = P_{H_2O}(II)$ represents the total contribution of both oxide-ion and proton. When the $P_{O_2}(I) = P_{O_2}(II)$, the EMF of water vapor concentration cell gives the protonic contribution in wet air.

3. Results and discussion

3.1. Structural and morphological characterization

Fig. 1 shows powder X-ray diffraction patterns at room temperature of undoped and Zn^{2+}-doped SnP_2O_7 ceramic samples sintered at 1200 °C for 5 h. It can be seen that the peaks are almost identical to those reported for SnP_2O_7 with a cubic or pseudo-cubic structure, in which SnO_6 octahedra units at the corners and P_2O_7 units at the edges share oxygen atoms at the corners [27]. It can also be seen that for the sample of x = 0.12, the impurity peak appears. Therefore, the doping limit of Zn^{2+} in SnP_2O_7 is at least x = 0.09.

Table 1 summarizes the lattice parameter and the unit cell volume of $Sn_{1-x}Zn_xP_2O_7$ (x = 0, 0.03, 0.06, 0.09, 0.12). It can be seen from Table 1 that the lattice parameter increases with increasing Zn^{2+} content, thus, resulting in the increases in unit cell volume. This variation is attributable to the higher ionic radius of Zn^{2+} (0.074 nm) compared with that of Sn^{4+} (0.069 nm) [28]. The ceramic sample of x = 0.09 shows the maximum lattice parameter, whereas the sample of x = 0.12 shows the smallest lattice parameter among the determined samples. The significant decrease in lattice parameter of x = 0.12 sample is likely due to the formation of impurity.

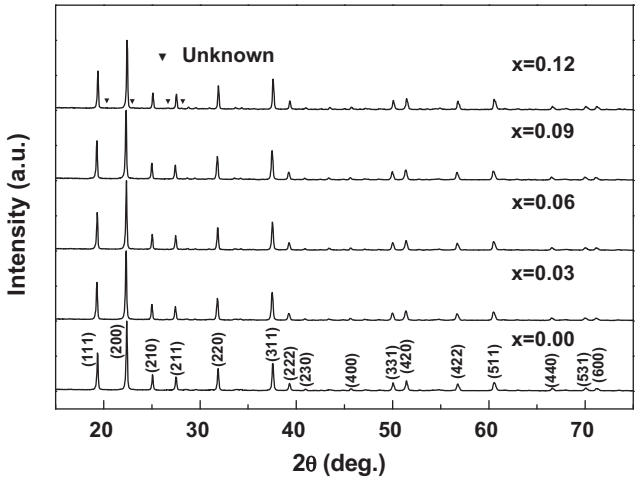

Fig. 1. XRD patterns of undoped and Zn^{2+}-doped SnP_2O_7 ceramic samples sintered at 1200 °C for 5 h.

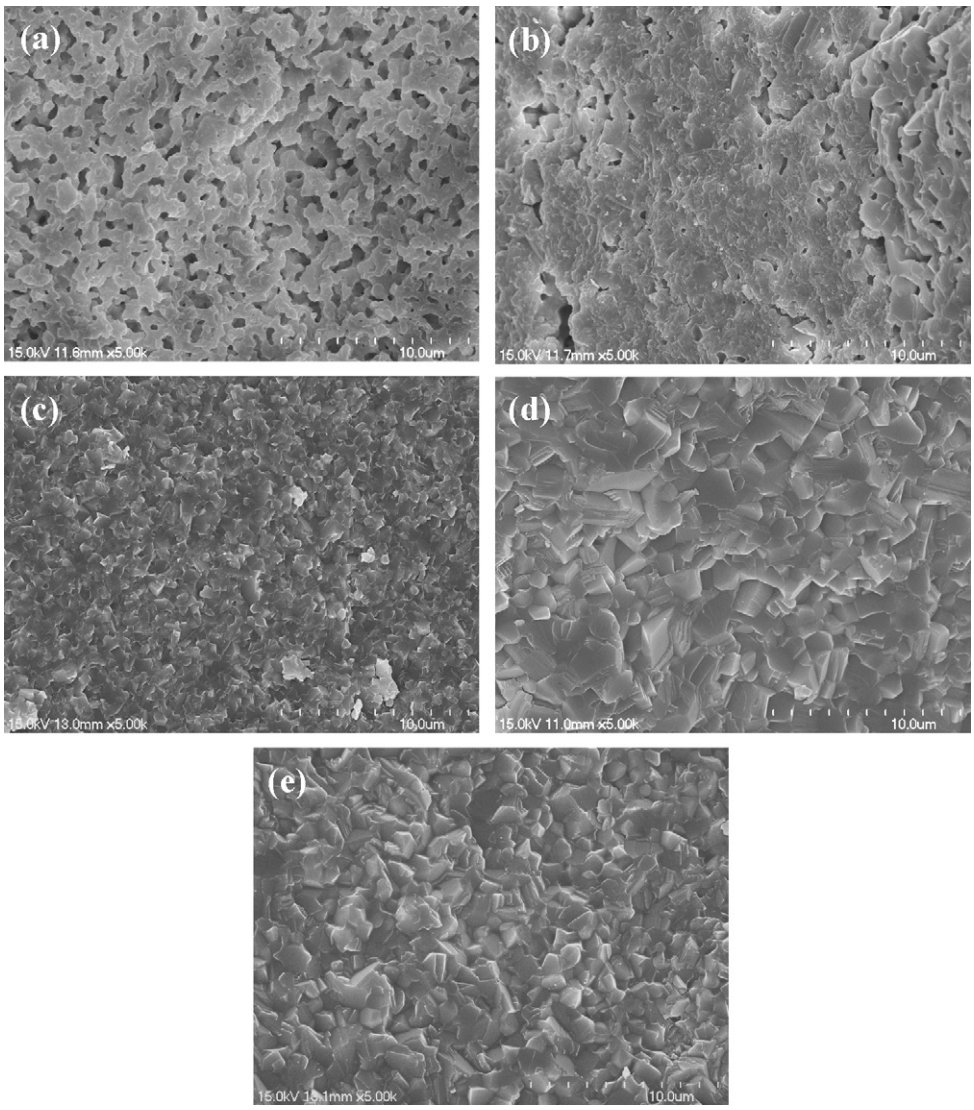

Fig. 2. SEM micrographs of the fracture surfaces for $Sn_{1-x}Zn_xP_2O_7$ ceramic samples of (a) $x = 0$; (b) $x = 0.03$; (c) $x = 0.06$; (d) $x = 0.09$ and (e) $x = 0.12$ sintered at 1200 °C.

Fig. 2 displays the SEM micrographs of fracture surfaces of the ceramic samples sintered at 1200 °C. A large number of pores are observed in the undoped SnP_2O_7 sample shown in Fig. 2 (a), indicating poor sintering behavior of the sample of $x = 0$. This is similar to the case in which porous rather than dense Zn^{2+}-doped SnP_2O_7 ceramics sintered at 1000 °C were obtained in this study. It can be seen from Fig. 2 (b)–(e) that when the Zn^{2+} doping content is increased, better densification is achieved in the ceramic samples, especially in the ceramic samples of $x \geq 0.09$. The enhanced densification with Zn^{2+} doping content increasing is also consistent with the result of total linear shrinkage measured in this study. The total linear shrinkage dramatically increases in the range from 0 to 9 mol% ZnO and a maximum linear shrinkage value of 15.6% (as compared with only 2.9% for the sample of $x = 0$) is achieved at $x = 0.09$. The relative densities for the samples of $x = 0.09$ and 0.12 are 86.6% and 91.7%, respectively. The above results by SEM observation and linear shrinkage measurement verify that the Zn^{2+} doping on Sn^{4+} site has a positive effect on the densification of SnP_2O_7 ceramics. The linear shrinkage/densification was likely attributable to the generation of oxygen vacancies [29] and will be further discussed below.

Table 1
Lattice parameter and unit cell volume of the $Sn_{1-x}Zn_xP_2O_7$ ($x = 0$, 0.03, 0.06, 0.09, 0.12) ceramic samples.

Zn content	Lattice parameter (nm)	Unit cell volume (nm^3)
x	a	V
0.00	0.7937(1)	0.4999
0.03	0.7942(3)	0.5009
0.06	0.7949(1)	0.5022
0.09	0.7951(2)	0.5026
0.12	0.7934(5)	0.4994

3.2. Electrical conductivity

Fig. 3 shows the total conductivities of $Sn_{1-x}Zn_xP_2O_7$ ($x = 0$, 0.03, 0.06, 0.09, 0.12) in wet air and wet hydrogen atmospheres. It is clear that the conductivities increased in the order: $x = 0.12 < x = 0.00 < x = 0.03 < x = 0.06 < x = 0.09$. The highest conductivities were observed for the $Sn_{0.91}Zn_{0.09}P_2O_7$ sample to be 1.69×10^{-4} S cm^{-1} in wet air and 1.91×10^{-4} S cm^{-1} in wet hydrogen at 600 °C. It is obvious that the substitution of Zn^{2+} for Sn^{4+} site plays an important role in the enhancement of conductivity. In comparison, the conductivity values previously reported [11,14–19] for the unsintered pellets prepared merely by pressing the doped tin pyrophosphate powders are about two orders of

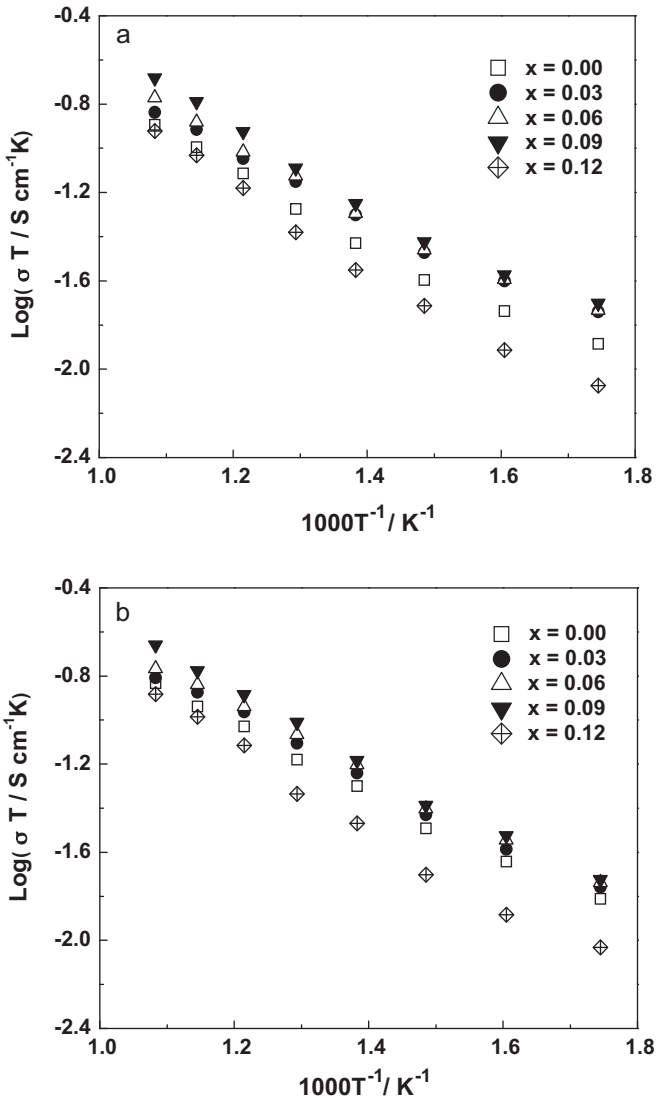

Fig. 3. Total conductivities of $Sn_{1-x}Zn_xP_2O_7$ (x = 0, 0.03, 0.06, 0.09, 0.12) ceramic samples in (a) wet air and (b) wet hydrogen atmospheres in the temperature range of 300–650 °C.

magnitude higher than our results. The higher conductivity values are attributed to the presence of leftover phosphoric acid in the unsintered pellets [22]. Tao [21] reported that $Sn_{0.92}In_{0.08}P_2O_{7-\delta}$ ceramic pellet by sintering the green pellet at 1000 °C shows a lower conductivity of 8×10^{-9} S cm^{-1} at 400 °C in air. This value is lower than our values, probably resulting from different dopants and prepared routes used. Phadke et al. [22] reported that dense $Sn_{0.9}Zn_{0.1}P_2O_{7-\delta}$ ceramic pellet was obtained through sintering the green pellet at 1400 °C, and that $Sn_{0.9}Zn_{0.1}P_2O_{7-\delta}$ showed a conductivity of 2.84×10^{-6} S cm^{-1} at 600 °C in unhumidified air. This conductivity value is about two orders of magnitude lower than our results for the ceramic samples sintered at 1200 °C. Obviously, the effect of sintering temperature on the conductivity is of the utmost importance. At sintering temperatures of 1000 °C or higher, the possibility of any leftover phosphoric acid from synthesis in these samples is eliminated [22]. However, too high sintering temperature may cause a fraction of phosphorus loss during the preparing process by vaporization and a partial disconnection of the P_2O_7 network for proton conduction, resulting in a large energy barrier for proton jumps between sites [14,22]. Therefore, taking into account both sinterability and conductivity, the sintering temperature in present investigation was selected to be 1200 °C, which could result in not only appropriate densities, but also high conductivities of ceramic samples.

As for the influence of Zn^{2+} doping level in SnP_2O_7 on the conductivities, as mentioned above, the conductivities first increased and then decreased with the Zn^{2+} doping level increasing. This may be interpreted as follows. The substitution of Zn^{2+} ion with lower ionic valance for Sn^{4+} ion in the lattice gives rise to oxygen vacancy due to charge compensation as indicated by the Eq. (5).

$$ZnO \xrightarrow{SnO_2} Zn''_{Sn} + O^{\times}_{O} + V^{\bullet\bullet}_{O} \quad (5)$$

Under oxygen-containing atmospheres the Eq. (6) may occur

$$\tfrac{1}{2}O_2 + V^{\bullet\bullet}_{O} \rightarrow O^{\times}_{O} + 2h^{\bullet} \quad (6)$$

When water vapor is introduced, as shown in Eqs. (7) and (8), the conduction of oxygen vacancy and electron hole decrease, at the same time, the proton conduction appears. In wet hydrogen, the proton conduction may be further enhanced according to the Eqs. (7)–(9)

$$H_2O(g) + V^{\bullet\bullet}_{O} + O^{\times}_{O} \rightarrow 2OH^{\bullet}_{o} \quad (7)$$

$$H_2O(g) + 2h^{\bullet} + 2O^{\times}_{O} \rightarrow 2OH^{\bullet}_{o} + \tfrac{1}{2}O_2 \quad (8)$$

$$H_2 + 2O^{\times}_{O} \rightarrow 2OH^{\bullet}_{o} + 2e' \quad (9)$$

The influence of Zn^{2+} doping level on the conductivities may be attributed to the effective concentration oxygen vacancy concentration and impurity phase [15,16]. It can be seen from Eq. (5) that the effective oxygen vacancy concentration may increase with increasing the Zn^{2+} doping level. Nevertheless, the concentrations of point defect pairs, $Zn''_{Sn}V^{\bullet\bullet}_{o}$ and $OH^{\bullet}_{o}Zn''_{Sn}OH^{\bullet}_{o}$, which resulted from the coulombic attraction among the point defects with opposite charges, may also increase at the same time, resulting in decrease in the effective oxygen vacancy concentration. Considering the opposite two factors above, the effective concentration of oxygen vacancy may reach its maximum value at x = 0.09. As a result, the highest conductivities 1.69×10^{-4} S cm^{-1} in wet air and 1.91×10^{-4} S cm^{-1} in wet hydrogen at 600 °C were observed for the sample of x = 0.09.

The H/D isotope effect on the conductivity is usually used as an evidence of the proton conduction in the samples [14,30]. The isotope effect may be estimated by the ratio of pre-exponential factors, A_D/A_H. Fig. 4 shows isotope effect on conductivity of $Sn_{0.91}Zn_{0.09}P_2O_7$ as a typical sample in argon saturated with H_2O

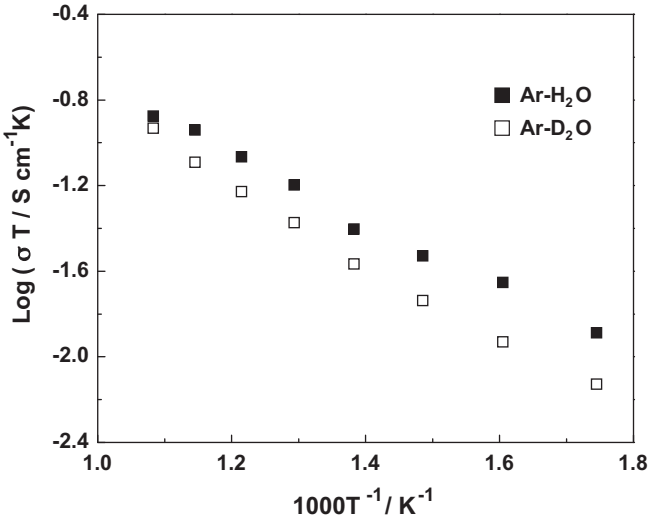

Fig. 4. Isotope effect on conductivity of $Sn_{0.91}Zn_{0.09}P_2O_7$ in argon saturated with H_2O or D_2O vapor at 25 °C.

or D_2O vapor at 25 °C. Obviously, the conductivity in H_2O–Ar atmosphere is higher than that in D_2O–Ar atmosphere. The A_D/A_H value is 1.456, which is close to $1 < \frac{A_D}{A_H} < \sqrt{2}$ [31]. In addition, the activation energy in the temperature range of 300–650 °C is also subjected to the H/D isotope effect. The activation energy in D_2O–Ar atmosphere (34.6 kJ/mol) is higher than that in H_2O–Ar atmosphere (29.8 kJ/mol), indicating that the ceramic sample possesses proton conduction in water vapor-containing atmosphere. The similar results were also observed for the other samples in this study. Here, the interaction (Eqs. (7) and (8)) between water vapor and oxygen vacancies (or electron holes) may be responsible for proton conduction in the ceramic sample [32]. When the dissociation of the O–H bond is a rate-determining step for proton conduction, the activation energy for D^+ is higher than that for H^+ by a difference in zero point energy of 0.05 eV (4.83 kJ/mol) [14], which is near our result.

3.3. Transference numbers of charge carriers

Fig. 5 (a) shows electromotive forces (EMFs) of hydrogen concentration cell for typical ceramic sample of $x = 0.09$. Dotted line indicates the theoretical values and symbol ■ represents the observed values of the hydrogen concentration cell. It can be seen that each observed value, EMF_{obs}, is close to the corresponding theoretical EMF_{cal}. The ionic transference numbers ($t_{ion} = 0.90$–0.95) are close to unity, indicating that this ceramic sample is almost a pure ionic conductor.

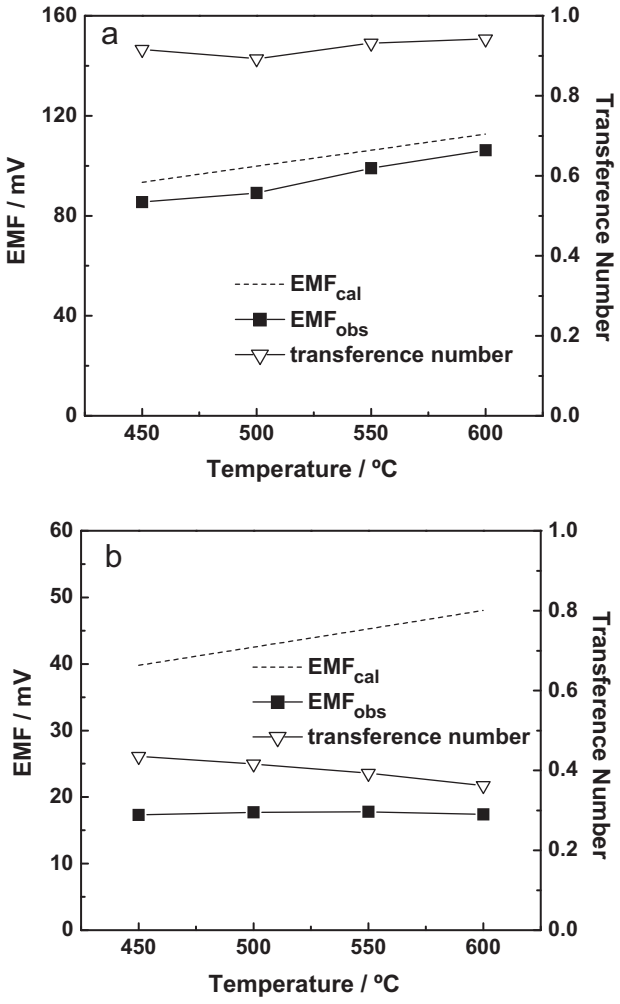

Fig. 5. EMF values of (a) hydrogen concentration cell and (b) water vapor concentration cell using the $Sn_{0.91}Zn_{0.09}P_2O_7$ ceramic as an electrolyte at 450–600 °C.

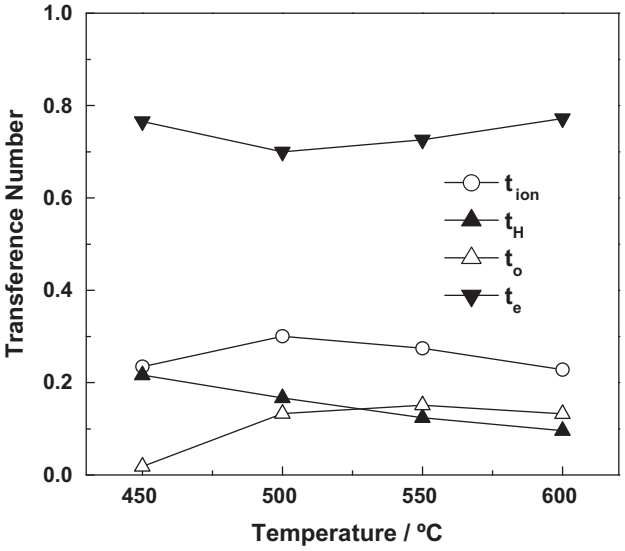

Fig. 6. Transference numbers of charge carriers in $Sn_{0.91}Zn_{0.09}P_2O_7$ in wet air atmosphere at 450–600 °C.

The oxide-ion contribution is confirmed from the EMF values of the water vapor concentration cell, because the hydrogen partial pressure is no longer imposed between the two electrodes [26]. The results are shown in Fig. 5 (b). Dotted line indicates the theoretical values and symbol ■ represents the observed values of the water vapor concentration cell. The oxide ionic transference numbers (t_O) are 0.36–0.43 at 450–600 °C, indicating the existence of oxide-ion conduction. Thus, the protonic ($t_H = t_{ion} - t_O$) and electronic ($t_e = 1 - t_{ion}$) transference numbers are evaluated from hydrogen as well as the water vapor concentration cells to be 0.47–0.59 and 0.05–0.10, respectively. The ionic conduction in the sample is contributed mainly to proton and partially to oxide-ion in wet hydrogen atmosphere from 450 °C to 600 °C. The other ceramic sample also showed similar conduction.

The ionic contribution under wet air atmosphere was examined using oxygen and water vapor concentration cells. Fig. 6 shows the transference numbers of charge carriers estimated from the EMF values of the concentration cells. The total ionic transference numbers (t_{ion}) and the protonic transference numbers (t_H) are 0.22–0.30 and 0.09–0.21, respectively. Thus, the oxide ionic transference numbers ($t_O = t_{ion} - t_H$) are calculated to be 0.02–0.15, the rest are electron hole transference numbers ($t_h = 0.69$–0.77). The conduction in the sample is contributed mainly to electron hole and partially to ion in wet air atmosphere at 450–600 °C.

The variation in protonic and oxide ionic transference numbers in wet air and hydrogen atmospheres may be interpreted according to the Eqs. (6)–(9). It can be seen from the Eqs. (6) and (8) that the conductivity and transference number of oxide-ion increase with oxygen partial pressure increasing. In other words, the conductivity and transference number of proton increase with hydrogen partial pressure increasing, resulting from the Eqs. (7)–(9).

4. Conclusions

Ceramic samples $Sn_{1-x}Zn_xP_2O_7$ ($x = 0$, 0.03, 0.06, 0.09, 0.12) have been prepared by a conventional solid state reaction method. It was found that all the ceramic samples exhibited a single phase structure except the ceramic sample of $x = 0.12$, the doping limit of Zn^{2+} in SnP_2O_7 was at least $x = 0.09$. The sintering temperature is a crucial effect on performances of the ceramic samples.

The sintering temperature applied to the present investigation was 1200 °C, which could result in not only appropriate densities, but also high conductivities of ceramic samples. The highest conductivities were observed for the $Sn_{0.91}Zn_{0.09}P_2O_7$ ceramic sample to be 1.69×10^{-4} S cm^{-1} in wet air and 1.91×10^{-4} S cm^{-1} in wet hydrogen at 600 °C. In wet hydrogen atmosphere, $Sn_{0.91}Zn_{0.09}P_2O_7$ was almost a pure ionic conductor, and the proton and oxide-ion transference numbers were 0.47–0.59 and 0.36–0.43, respectively. Whereas in wet air atmosphere, the ceramic sample was a mixed ion and electron hole conductor, and the conduction was contributed mainly to electron hole and partially to ion. The ceramic sample $Sn_{0.91}Zn_{0.09}P_2O_7$ may be a potential electrolyte candidate for intermediate temperature fuel cell.

Acknowledgements

This work was supported by the National Natural Science Foundation of China (No. 20771079) and funded by the Priority Academic Program Development of Jiangsu Higher Education Institutions.

References

[1] B.C.H. Steele, A. Heinzel, Nature 414 (2001) 345–352.
[2] S.M. Haile, D.A. Boysen, C.R.I. Chisholm, R.B. Merle, Nature 410 (2001) 910–913.
[3] T. Norby, Nature 410 (2001) 877–878.
[4] S.W. Tao, J.T.S. Irvine, Adv. Mater. 18 (2006) 1581–1584.
[5] K. Xie, R.Q. Yan, X.R. Chen, S.L. Wang, Y.Z. Jiang, X.Q. Liu, G.Y. Meng, J. Alloys Compd. 473 (2009) 323–329.
[6] B. Lin, Y.C. Dong, S.L. Wang, D.R. Fang, H.P. Ding, X.Z. Zhang, X.Q. Liu, G.Y. Meng, J. Alloys Compd. 478 (2009) 590–593.
[7] H. Zhong, H. Matsumoto, T. Ishihara, A. Toriyama, J. Power Sources 186 (2009) 238–243.
[8] A.M. Amesti, A. Larranaga, L.M.R. Martínez, M.L. Nó, J.L. Pizarro, A. Laresgoiti, M.I. Arriortua, J. Power Sources 192 (2009) 151–157.
[9] L. Zhao, B.B. He, Q. Nian, Z.Q. Xun, R.R. Peng, G.Y. Meng, X.Q. Liu, J. Power Sources 194 (2009) 291–294.
[10] Y.Z. Li, T. Kunitake, Y. Aoki, E. Muto, Adv. Mater. 20 (2008) 2398–2404.
[11] X. Wu, A. Verma, K. Scott, Fuel Cells 8 (2008) 453–458.
[12] J. Otomo, N. Minagawa, C. Wen, K. Eguchi, H. Takahashi, Solid State Ionics 156 (2003) 357–369.
[13] D.A. Boysen, S.M. Haile, H.J. Liu, R.A. Secco, Chem. Mater. 15 (2003) 727–736.
[14] M. Nagao, T. Kamiya, P. Heo, A. Tomita, T. Hibino, M. Sano, J. Electrochem. Soc. 153 (2006) A1604–A1609.
[15] H.T. Wang, J.W. Liu, W.B. Wang, G.L. Ma, J. Power Sources 195 (2010) 5596–5600.
[16] H.T. Wang, H.M. Zhang, G.X. Xiao, F. Zhang, T. Yu, J. Xiao, G.L. Ma, J. Power Sources 196 (2011) 683–687.
[17] A. Tomita, N. Kajiyama, T. Kamiya, M. Nagao, T. Hibino, J. Electrochem. Soc. 154 (2007) B1265–B1269.
[18] K. Genzaki, P. Heo, M. Sano, T. Hibino, J. Electrochem. Soc. 156 (2009) B806–B810.
[19] Y.C. Jin, Y.B. Shen, T. Hibino, J. Mater. Chem. 20 (2010) 6214–6217.
[20] R. Lan, S.W. Tao, J. Alloys Compd. 486 (2009) 380–385.
[21] S.W. Tao, Solid State Ionics 180 (2009) 148–153.
[22] S.R. Phadke, C.R. Bowers, E.D. Wachsman, J.C. Nino, Solid State Ionics 183 (2011) 26–31.
[23] X.X. Xu, S.W. Tao, P. Wormald, J.T.S. Irvine, J. Mater. Chem. 20 (2010) 7827–7833.
[24] Y.B. Shen, M. Nishida, W. Kanematsu, T. Hibino, J. Mater. Chem. 21 (2011) 663–670.
[25] T. Hibino, J. Ceram. Soc. Japan 119 (2011) 677–686.
[26] J. Guan, S.E. Dorris, U. Balachandran, M. Liu, Solid State Ionics 100 (1997) 45–52.
[27] R.K.B. Gover, N.D. Withers, S. Allen, R.L. Withers, J.S.O. Evans, J. Solid State Chem. 166 (2002) 42–48.
[28] R.D. Shannon, Acta Crystallogr. A 32 (1976) 751.
[29] C.R. Foschini, L. Perazolli, J.A. Varela, J. Mater. Sci. 39 (2004) 5825–5830.
[30] M. Nagao, A. Takeuchi, P. Heo, T. Hibino, M. Sano, A. Tomita, Electrochem. Solid State Lett. 9 (2006) A105–A109.
[31] A.S. Nowick, A.V. Vaysleyb, Solid State Ionics 97 (1997) 17–26.
[32] X.L. Chen, C.S. Wang, E.A. Payzant, C.R. Xia, D. Chu, J. Electrochem. Soc. 155 (2008) B1264–B1269.